Supporting Information for

Anthropogenic dust as a significant source of ice-nucleating particles in the urban environment

Jie Chen[1,2], Zhijun Wu[1,*], Xianda Gong[3,4], Yanting Qiu[1], Shiyi Chen[1], Limin Zeng[1], Min Hu[1]

1State Key Joint Laboratory of Environmental Simulation and Pollution Control, College of Environmental Sciences and Engineering, Peking University, Beijing, China

2Institute for Atmospheric and Climate Science, ETH Zürich, Zurich, 8092, Switzerland

3Key Laboratory of Coastal Environment and Resources of Zhejiang Province, School of Engineering, Westlake University, Hangzhou, Zhejiang Province, 310030, China

4Center for Aerosol Science and Engineering, Department of Energy, Environmental and Chemical Engineering, Washington University in St. Louis, MO, USA

Contents of this file

Introduction

The Supporting Information shows additional figures (S1~S10) and tables (S1~S3) to provide detailed sampling information and other physicochemical characterizations of aerosols and ice nucleating particles in the present study.

Table S1. The sampling information of the filter samples

Sampling Date	Starting time*	Ending time	Air volume (L)	$PM_{2.5}$ (μg m^{-3})	PM_{10} (μg m^{-3})
2020/06/22	9:32	9:21	42870	66.3±22.9	87.7±28.6
2020/07/03	9:47	9:43	43080	58.8±24.6	68.5±30.5
2020/07/12	11:23	9:21	39540	108.0±31.4	136.7±35.7
2020/07/13	9:36	9:25	42870	53.2±22.0	79.2±25.1
2020/07/14	9:57	9:29	42360	38.4±9.8	61.2±12.9
2020/07/15	9:46	9:24	42540	35.6±9.1	57.8±12.8
2020/07/16	9:41	9:27	42780	60.6±22.1	86.8±22.2

2020/07/21	9:45	9:13	42240	44.6±12.3	73.1±18.0

*The sampling time is Beijing time (UTC +8 hours)

Table S2. The correlation between the number concentration of INP (N_{INP}) and particles with different sizes ($N_{>*}$)

The number concentration of particles larger than * μm ($N_{>*}$)	R^2: correlation between $N_{>*}$ and N_{INP}	
	Total N_{INP}	Heat-resistant N_{INP}
$N_{>500\ nm}$	0.37	0.51
$N_{>1\ \mu m}$	0.50	0.67
$N_{>1.8\ \mu m}$	0.20	0.28

Table S3. Element concentrations of particles in different size

Date	Na	Mg	Al	K	Ca	Mn	Fe	Zn	As	Ba	Pb	others
D_{50}=3.2 μm (μg/L)												
6/22	1217.4	1325.3	1443.0	507.3	6473.0	61.1	1762.8	95.6	2.4	61.8	16.6	244.1
7/03	766.2	979.1	782.7	383.6	4422.0	38.7	1392.0	98.2	1.5	54.1	13.2	213.1
7/12	638.9	1194.8	972.9	601.3	5317.4	51.9	1833.3	149.6	3.4	75.1	22.2	293.9
7/13	300.3	1260.1	1115.4	452.9	5478.9	49.1	1648.0	80.6	2.6	56.1	13.6	245.8
7/14	336.8	1546.5	1309.2	480.6	6550.4	48.8	1803.5	80.7	1.6	74.0	13.0	203.1
7/15	237.0	861.5	747.2	320.1	4118.6	30.8	977.7	70.2	1.6	44.6	8.1	159.8
7/16	435.5	1554.1	2009.6	671.4	7841.1	63.7	2171.4	136.1	2.4	82.7	43.0	344.8
7/21	535.4	1556.3	1640.4	556.9	7201.9	68.3	2510.6	109.6	2.7	81.5	18.9	296.4
D_{50}=0.56 μm (μg/L)												
6/22	317.5	59.9	238.5	665.2	213.2	49.1	466.6	132.8	8.2	6.6	33.8	68.1
7/03	366.6	31.4	244.3	590.2	144.8	46.0	307.3	179.4	8.6	7.4	36.8	118.2
7/12	426.3	46.8	439.0	724.6	268.5	61.1	510.9	255.5	15.9	8.0	55.6	105.7
7/13	289.3	51.6	86.0	464.4	343.4	36.4	373.8	120.5	13.8	6.9	29.1	53.5
7/14	198.4	73.4	115.5	383.1	1206.3	43.9	461.2	147.1	13.4	7.4	26.1	77.2
7/15	200.4	62.4	122.4	412.8	221.0	39.2	438.5	120.2	8.4	8.6	25.3	61.4
7/16	372.1	60.0	134.3	929.3	251.9	54.0	482.7	268.6	16.4	11.4	77.6	170.6
7/21	325.3	54.1	131.0	642.0	293.7	48.2	460.7	193.5	8.9	7.5	53.6	82.0

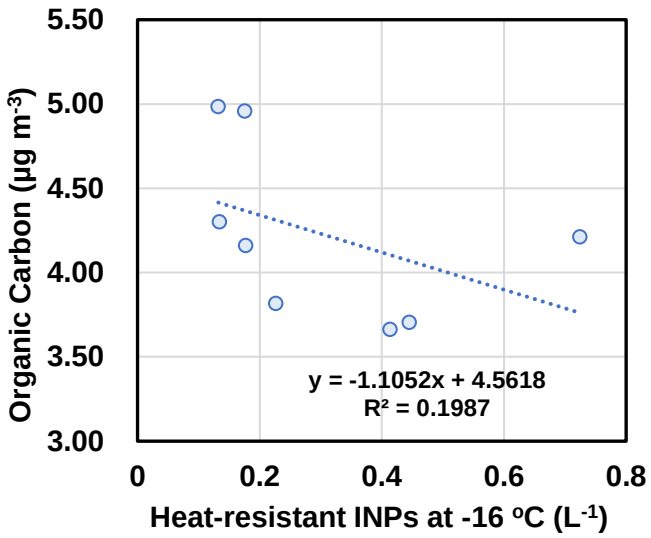

Figure S1. The correlation between heat-resistant N_{INP} at -16 °C and organic carbon (OC) measured by the Sunset ECOC analyzer.

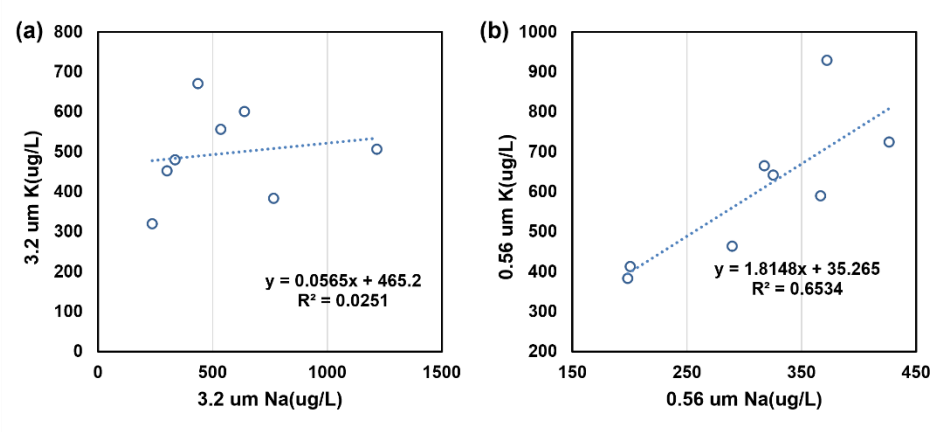

Figure S2. The correlations between the Na and K mass concentrations in 3.2 µm (a) and 0.56 µm (b) particles.

Text S1. The strong correlation between Na and K in fine particles (R^2=0.65) proved that they come from the same anthropogenic source such as biomass burning and industrial emissions, as supported by previous studies [*Lian et al.*, 2022; *Ooki et al.*, 2002]. This correlation became very weak in coarse particles (R^2=0.02) where Na was commonly found in natural sources (such as the sea-salt NaCl in marine aerosol). This result indicates that compared to coarse particles, fine particles are influenced by anthropogenic sources.

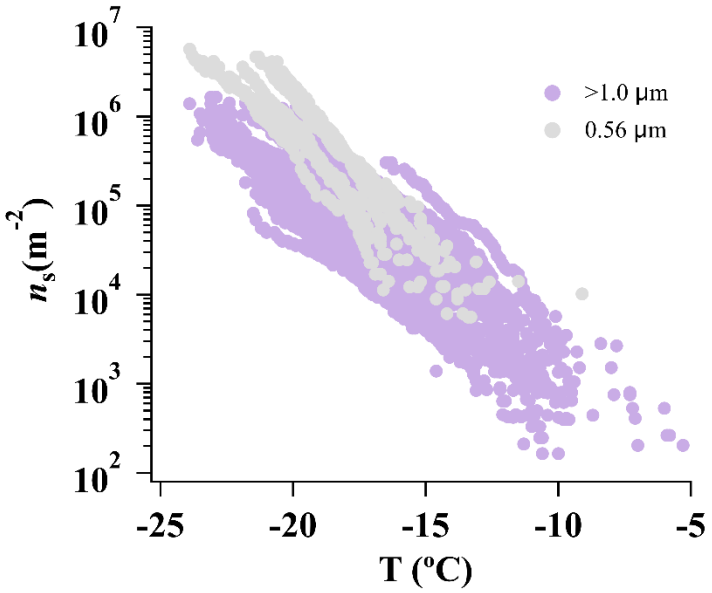

Figure S3. The cumulative number concentration of the ice active sites per unit surface area (n_s) of particles in different sizes. Particles larger than 1 µm include particles with D_{50} sizes of 1 µm, 1.8 µm, 3.2 µm and 5.6 µm.

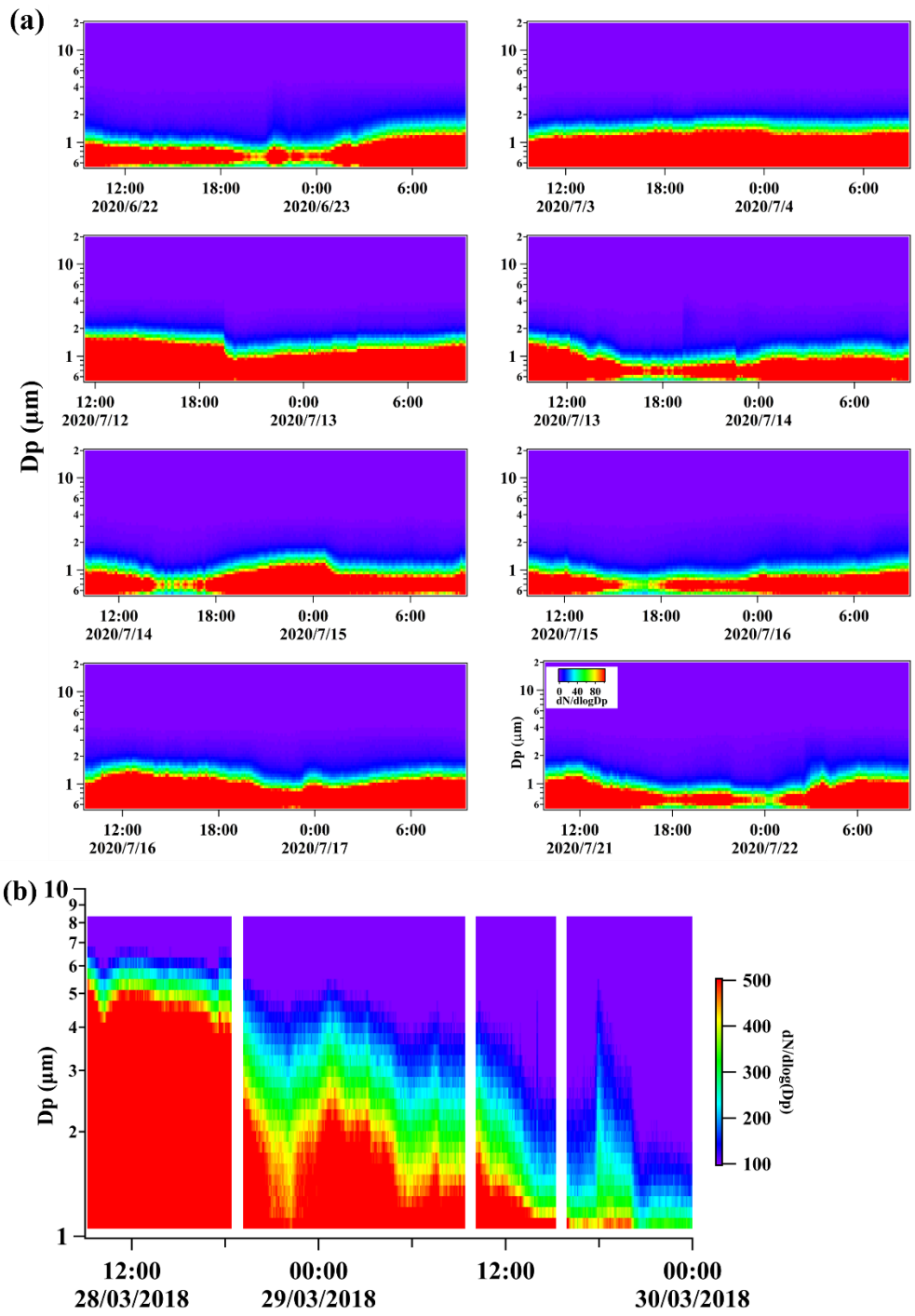

Figure S4. The time series of the aerodynamic size (Dp) distribution of aerosols from 0.542 μm to 19.81 μm measured during each sampling day (a) and compared with those detected during the dust event (b) by *Chen et al.* [2021]. The unit of dN/dlog(Dp) is cm^{-3}.

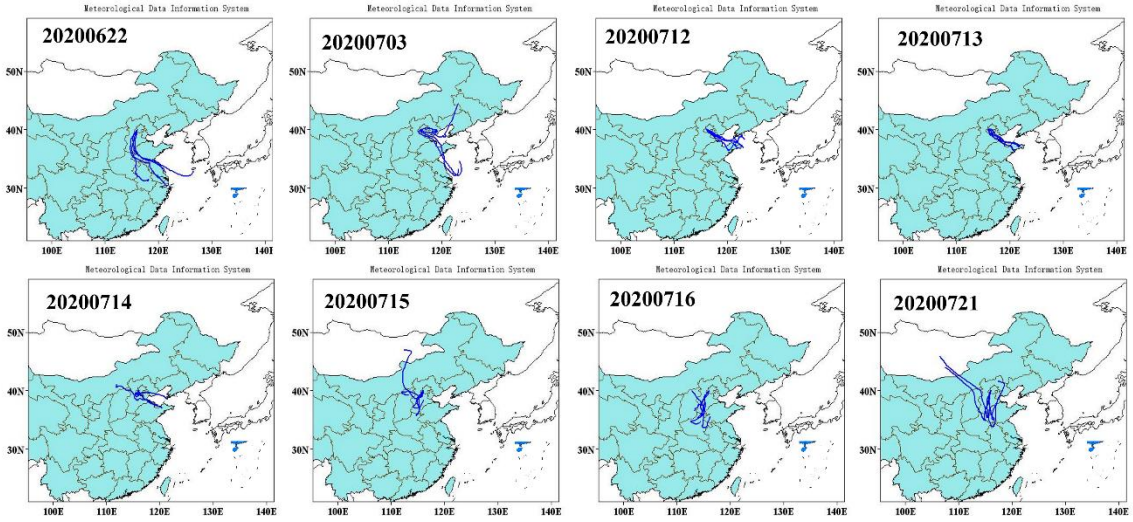

Figure S5. The 72 hours backward trajectories of air masses during the sampling time. Each trajectory was calculated every 6 hours, resulting in 4 trajectories for each sample (sampling for 24 hours) calculated at 1:00, 7:00, 13:00, and 19:00 UTC.

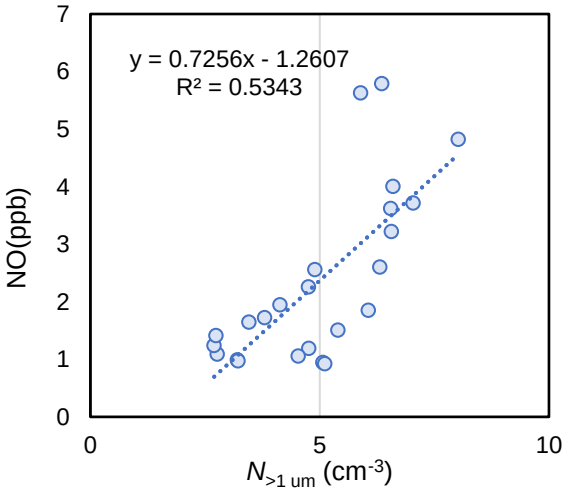

Figure S6. The hourly mean concentration of nitric oxide (NO) and the hourly mean number concentration of coarse particles during the sampling time. One data point represents the mean value of NO detected at the same time on different days (24 data points indicate 24 hours of the day).

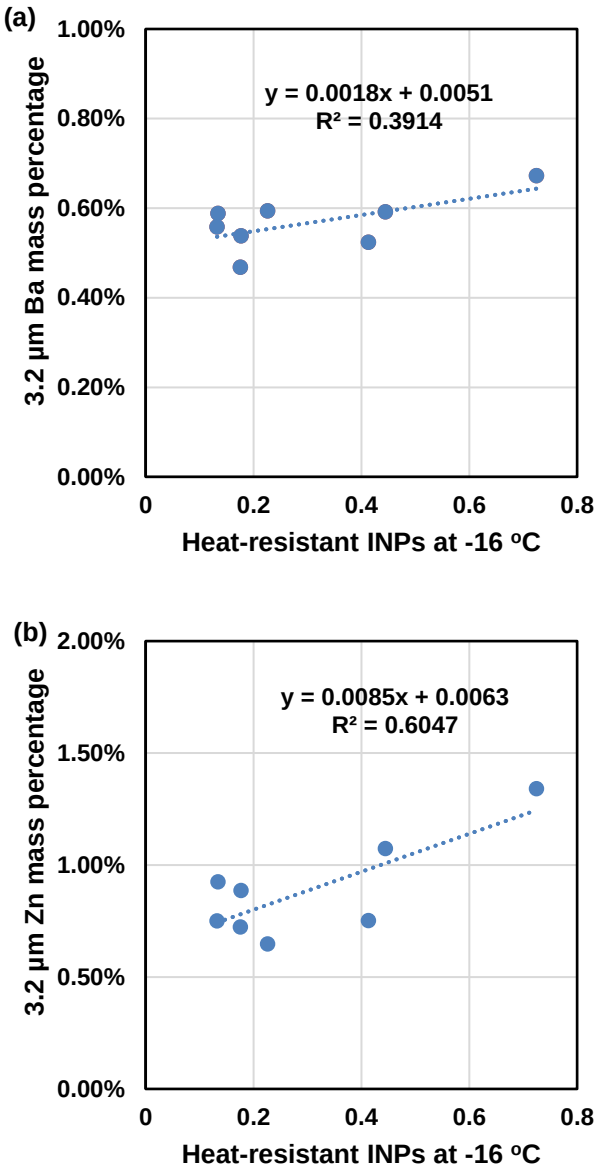

Figure S7. The correlations between the heat-resistant N_{INP} and the mass percentages of Ba (a) and Zn (b) in D_{50}=3.2 μm particles.

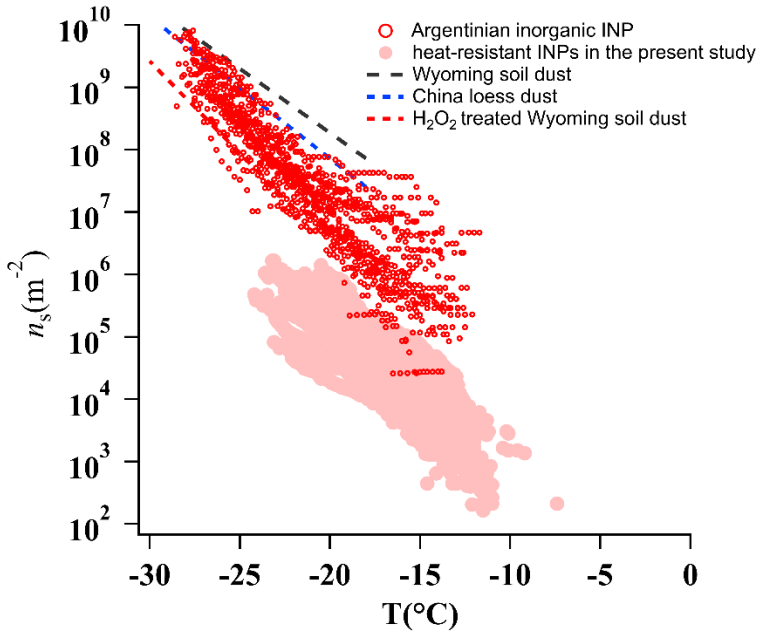

Figure S8. The comparison of n_s from the present study (purple circles) and those from the soil dust measured by *Tobo et al.* [2014] and inorganic INPs influenced by Argentinian land surface emission in *Testa et al.* [2021]. Note that the unit of n_s in *Tobo et al.* [2014] was cm^{-2} while here we converted the data to m^{-2}.

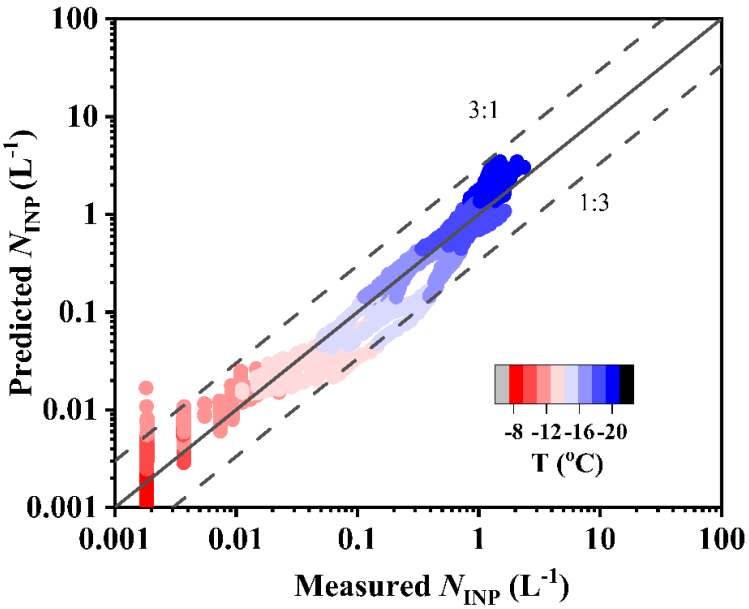

Figure S9. The comparison of N_{INP} from the observation and predicted by the newly developed parameterization in the present study.

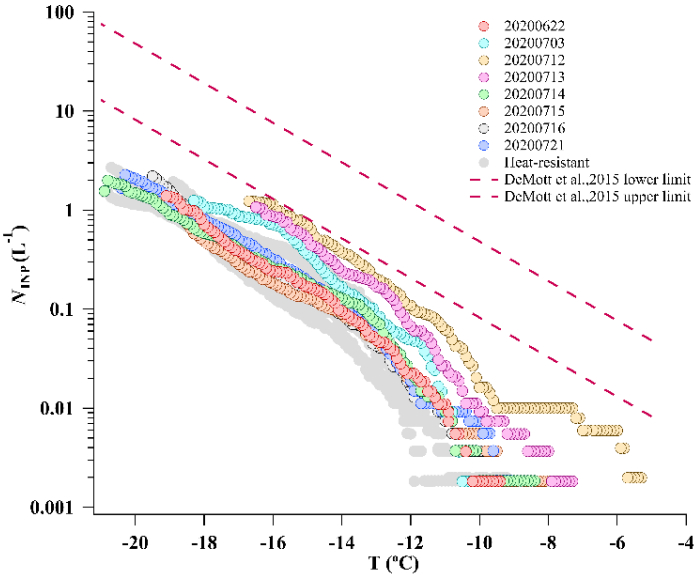

Figure S10. The number concentration of INPs (N_{INP}) as a function of temperatures measured during the sampling time; The gray circles represent the number concentration of heat-resistant INPs after being heated at 95 °C for 20 mins. The pink dashed lines represent the upper and lower limits of INPs estimated according to the parameterization proposed by *DeMott et al.* [2015] based on the highest and the lowest number concentrations of particles larger than 500 nm detected in the present study.

Reference

Chen, J., Z. Wu, J. Chen, N. Reicher, X. Fang, Y. Rudich, and M. Hu (2021), Size-resolved atmospheric ice-nucleating particles during East Asian dust events, *Atmos. Chem. Phys.*, 21(5), 3491-3506.

DeMott, P. J., Prenni, A. J., McMeeking, G. R., Sullivan, R. C., Petters, M. D., Tobo, Y., et al. (2015), Integrating laboratory and field data to quantify the immersion freezing ice nucleation activity of mineral dust particles, *Atmos. Chem. Phys.*, 15(1), 393–409.

Lian, X., G. Tang, X. Dao, X. Hu, X. Xiong, G. Zhang, Z. Wang, C. Cheng, X. Wang, and X. Bi (2022), Seasonal variations of imidazoles in urban areas of Beijing and Guangzhou, China by single particle mass spectrometry, *Sci. Total. Environ.*, 844, 156995.

Ooki, A., M. Uematsu, K. Miura, and S. Nakae (2002), Sources of sodium in atmospheric fine particles, *Atmos. Environ.*, 36(27), 4367-4374.

Testa, B., Hill, T.C., Marsden, N.A., Barry, K.R., Hume, C.C., Bian, Q., Uetake, J., Hare, H., Perkins, R.J., Möhler, O. and Kreidenweis, S.M., (2021), Ice nucleating particle connections to regional Argentinian land surface emissions and weather during the Cloud, Aerosol, and Complex Terrain Interactions experiment. *J. Geophys. Res. Atmos.*, 126(23), p.e2021JD035186.

Tobo, Y., P. DeMott, T. Hill, A. Prenni, N. Swoboda-Colberg, G. Franc, and S. Kreidenweis (2014), Organic matter matters for ice nuclei of agricultural soil origin, *Atmos. Chem. Phys.*, 14(16), 8521-8531.